On the Performance of Cache-Free/Cache-Aided STBC-NOMA in Cognitive Hybrid Satellite-Terrestrial Networks

Vibhum Singh, *Member, IEEE*, Sourabh Solanki, *Member, IEEE*, Geoffrey Eappen,
Rakesh Palisetty, *Member, IEEE*, Thang X. Vu, *Senior Member, IEEE*,
Juan Carlos Merlano-Duncan, *Senior Member, IEEE*, Symeon Chatzinotas, *Senior Member, IEEE*,
and Björn Ottersten, *Fellow, IEEE*

Abstract—Future wireless networks pose several challenges such as high spectral efficiency, wide coverage, massive connectivity, low receiver complexity, etc. To this end, this letter investigates an overlay-based cognitive hybrid satellite-terrestrial network (CHSTN) combining non-orthogonal multiple access (NOMA) and conventional Alamouti space-time block coding (STBC) techniques. Herein, a decode-and-forward based secondary terrestrial network cooperates with a primary satellite network for dynamic spectrum access. Further, for reliable content delivery and low latency requirements, wireless caching is employed, whereby the secondary network can store the most popular contents of the primary network. Considering the relevant heterogeneous fading channel models and the NOMA-based imperfect successive interference cancellation, we examine the performance of CHSTN for the cache-free (CF) STBC-NOMA and the cache-aided (CA) STBC-NOMA schemes. We assess the outage probability expressions for primary and secondary networks and further, highlight the corresponding achievable diversity orders. Indicatively, the proposed CF/CA STBC-NOMA schemes for CHSTN perform significantly better than the benchmark standalone NOMA and OMA schemes.

Index Terms—Caching, hybrid satellite-terrestrial networks, non-orthogonal multiple access, overlay cognitive radio, space-time block coding.

I. INTRODUCTION

FUTURE wireless networks have to effectively satisfy the demands of ubiquitous coverage, high spectral efficiency, and massive connectivity. In this respect, cognitive hybrid satellite-terrestrial networks (HSTNs) incorporating non-orthogonal multiple access (NOMA) have gained significant research interest [1], [2]. However, in NOMA, recurrent superposition-successive interference cancellation (SIC) pair processing results in an increased complex receiver architecture. Thus, a unique design while employing the space-time block coding (STBC) is presented in [3], which dramatically reduces the number of SICs executed in the system. Moreover, in practice, it is highly challenging to obtain accurate channel state information (CSI) at the transmitter, especially in satellite communication (SATCOM) systems [4].

Consequently, the Alamouti STBC [5] technique can be exploited in the NOMA-based cognitive HSTNs (CHSTNs) to achieve full spatial transmit diversity. In this regard, by considering the heterogeneous fading channel models, authors in [6] and [7] employed the STBC technique in their analytical frameworks for the SATCOM system and HSTN, respectively.

Nevertheless, the escalating growth in mobile data traffic pushes more and more users from using traditional linear broadcasting services to non-linear streaming services like YouTube and NetFlix. Accordingly, SATCOMs can facilitate the wide area distribution of high-resolution content with reduced latency, while employing the wireless caching [8]. For this, it provides the popular contents directly to the end users without decoding but by storing them into routers, relays, etc., during the cache placement phase [9].

Inspired by the above research studies, in this letter, we characterize an overlay-based CHSTN for a downlink communication scenario between a primary satellite transmitter and its receiver with the aid of a decode-and-forward based secondary terrestrial network consisting of a single transmitter-receiver pair. Notably, the considered analytical framework deploys NOMA and conventional Alamouti STBC techniques for signal transmission. Moreover, the secondary transmitter (ST) has built-in cache capability to store the popular contents of the primary network while following the most popular content (MPC) based caching scheme [2]. In summary, 1) For the considered CHSTN, we first propose the cache-free (CF) STBC-NOMA and cache-aided (CA) STBC-NOMA schemes; 2) Then, anticipating the feasible implication of imperfect SIC (ipSIC), we quantify the performance of CHSTN for the proposed schemes. For this, we derive the outage probability (OP) expressions for the primary and secondary networks and thereafter, for comparison purposes, provide the Monte-Carlo simulations for the benchmark NOMA and OMA schemes without any caching and STBC techniques; 3) Finally, we examine the asymptotic outage performance of the primary and secondary networks under the proposed schemes at a high signal-to-noise ratio (SNR) and calculate their associated attainable diversity orders.

II. SYSTEM DESCRIPTION

A. System Model

Let us discuss the system model first for CHSTN under the CF STBC-NOMA scheme. Herein, a primary satellite transmitter-primary receiver (PR) pair coexists with a ST-secondary receiver (SR) pair, and are denoted as $S-D_p$ and $R-D_q$, respectively.[1]

---

[1]A practical scenario for CHSTN may constitute a source S corresponding to a geostationary orbit (GEO) satellite and node D_p representing the handheld device as integrated in Digital Video Broadcast-Satellite Handheld (DVB-SH) service (in S-band) [10], whereas the secondary nodes R and D_q could be femtocell users, not having a dedicated spectrum for their communication [2].

Based on the overlay approach, ST node *R* gets the authorization of spectrum access on a secondary basis in return for participating in primary cooperation on a priority basis. For this, we assume that the PR is assumed to be aware of the instantaneous CSI from node *R*. Accordingly, ST acts as a cooperative relay and employs the power-domain NOMA [1] while forwarding the primary signal and concurrently transmitting its own signal to SR. Further, a direct satellite link is assumed between nodes *S* and D_p. As such, primary transmitter (PT) and ST deploy the Alamouti STBC technique in their signal transmissions. PT is equipped with two transmit antennas (S_t^l), ST is equipped with two transmit and one receive antennas (R_t^l and R_r), $l \in \{1, 2\}$, whereas, PR and SR are provided with one receive antenna each, represented as D_{p_r} and D_{q_r}, respectively. Thus, the overall system is configured in such a way that the Alamouti 2×1 multiple-input-single-output (MISO) mode can be implemented for both the STBC transmissions from PT and ST. We assume that each channel experiences uncorrelated quasi-static block fading. Various channel coefficients related to satellite links follow shadowed-Rician fading and are marked as g_{si}^l, $i \in \{r, d_p, d_q\}$, whereas, channel coefficients for terrestrial links are represented as h_{rj}^l, $j \in \{d_p, d_q\}$, and are encountered to independent Nakagami-*m* fading distributions. All receiving nodes are likely to be subjected to additive white Gaussian noise (AWGN) with mean zero and variance σ^2.

B. Channel Model

For satellite links, following the shadowed-Rician fading model, the probability density function (PDF) of receive SNR $\Lambda_{si}^l = \tilde{\eta}_s |g_{si}^l|^2$ is given as [1], [2]

$$f_{\Lambda_{si}^l}(x) = \alpha_i^l \sum_{\kappa=0}^{m_{si}^l-1} \frac{\zeta^l(\kappa)}{(\tilde{\eta}_s)^{\kappa+1}} x^\kappa e^{-\left(\frac{\beta_i^l-\delta_i^l}{\tilde{\eta}_s}\right)x}, \qquad (1)$$

where $\tilde{\eta}_s = \frac{\eta_s}{2} = \frac{P_s}{2\sigma^2}$ with P_s being the transmit power through satellite *S*, which is equally divided between two transmit antennas. Further, $\alpha_i^l = (2b_{si}^l m_{si}^l/(2b_{si}^l m_{si}^l + \Omega_{si}^l))^{m_{si}^l}/2b_{si}^l$, $\beta_i^l = 1/2b_{si}^l$, $\delta_i^l = \Omega_{si}^l/(2b_{si}^l)(2b_{si}^l m_{si}^l + \Omega_{si}^l)$, with $2b_{si}^l$ and Ω_{si}^l are the respective average powers of multipath and line-of-sight components, m_{si}^l is the integer-valued fading severity parameter, and $\zeta^l(\kappa) = (-1)^\kappa (1 - m_{si}^l)_\kappa (\delta_i^l)^\kappa/(\kappa!)^2$ with $(\cdot)_\kappa$ representing the Pochhammer symbol [11, p. xliii].

The Nakagami-*m* fading for the terrestrial links yields the PDF of receive SNR $\Lambda_{rj}^l = \tilde{\eta}_r |h_{rj}^l|^2$ as in [2, eq. (6)], where $\tilde{\eta}_r = \frac{\eta_r}{2} = \frac{P_r}{2\sigma^2}$ and P_r is the transmit power through ST node *R*, which is equally distributed between the two transmit antennas, m_{rj}^l and Ω_{rj}^l are the corresponding fading severity parameter and average power, and $\Gamma(\cdot)$ represents the Gamma function [11, eq. (8.310.1)].

C. STBC-NOMA Signal Model

Under the CF STBC-NOMA scheme, the entire communication executes in two time phases, each with two time slots. During the Phase-I, satellite *S* transmits the unit energy signals $x_{d_{p_1}}$ and $x_{d_{p_2}}$ (obeying $\mathbb{E}[|x_{d_{p_1}}|^2] = \mathbb{E}[|x_{d_{p_2}}|^2] = 1$) in first time slot and $-x_{d_{p_2}}^*$ and $x_{d_{p_1}}^*$ in second time slot through antennas S_t^1 and S_t^2, respectively, where $\mathbb{E}[\cdot]$ denotes the expectation and * represents the complex conjugate operation. Accordingly, the received SNR at node *i*,

$i \in \{r, d_p, d_q\}$, can be expressed as $\Lambda_{si,x_{d_p}} = \Lambda_{si}^1 + \Lambda_{si}^2$, where x_{d_p} is used in subscript to indicate the equivalent SNR corresponding to the primary signal. If ST node *R* is able to decode both signals $x_{d_{p_1}}$ and $x_{d_{p_2}}$ successfully, it superimposes them during the Phase-II with its own signals and generates the signals z_{r_1} and z_{r_2} in first time slot and $-z_{r_2}^*$ and $z_{r_1}^*$ in second time slot through antennas R_t^1 and R_t^2, respectively. Here, $z_{r_1} = \sqrt{\frac{(1-\rho)P_r}{2}} x_{d_{p_1}} + \sqrt{\frac{\rho P_r}{2}} x_{d_{q_1}}$ and $z_{r_2} = \sqrt{\frac{(1-\rho)P_r}{2}} x_{d_{p_2}} + \sqrt{\frac{\rho P_r}{2}} x_{d_{q_2}}$, with $\rho \in (0, 0.5)$ being the power allocation factor which is judiciously chosen to allocate more power towards the weak NOMA (far-away) user D_p, complying with $|h_{rd_p}^l|^2 \leq |h_{rd_q}^l|^2$ [1]. Hereby, relying on the NOMA principle, user D_p decodes its signal directly. Thus, the received signal-to-interference-plus-noise ratio (SINR) at node D_p is followed as

$$\Lambda_{rd_p,x_{d_p}} = \frac{(1-\rho)\left(\Lambda_{rd_p}^1 + \Lambda_{rd_p}^2\right)}{\rho\left(\Lambda_{rd_p}^1 + \Lambda_{rd_p}^2\right) + 1}. \qquad (2)$$

Next, strong NOMA (nearby) user D_q executes the SIC operation to first decode the primary signal x_{d_p}. Accordingly, the received SINR at D_q can be given as

$$\Lambda_{rd_q,x_{d_p}} = \frac{(1-\rho)\left(\Lambda_{rd_q}^1 + \Lambda_{rd_q}^2\right)}{\rho\left(\Lambda_{rd_q}^1 + \Lambda_{rd_q}^2\right) + 1}. \qquad (3)$$

Based on the above SINR, user D_q tries to cancel the primary interference received during Phase-I. Consequently, the SINR at user D_q can be obtained as

$$\Lambda_{rd_q,x_{d_q}} = \frac{\rho\left(\Lambda_{rd_q}^1 + \Lambda_{rd_q}^2\right)}{(1-\rho)\left(\Lambda_{D_q}^1 + \Lambda_{D_q}^2\right) + 1}, \qquad (4)$$

where the term $\Lambda_{D_q}^l = \tilde{\eta}_r |h_{D_q}^l|^2$ in the denominator arises due to the SIC error propagation, whose channel coefficient $h_{D_q}^l$ is subjected to Nakagami-*m* fading with corresponding fading severity parameter and average channel power gain as $m_{D_q}^l$ and $\Omega_{D_q}^l$ [2]. The PDF of $\Lambda_{D_q}^l$ can be referred from [2, eq. (6)] with some manipulations.

On the contrary, ST remains silent in case of unsuccessful decoding of the primary signals $x_{d_{p_1}}$ and $x_{d_{p_2}}$ in Phase-I [12]. Since the primary network's minimum rate requirement may not be satisfied in this case, the secondary users will not be allowed to access the licensed spectrum.

D. Caching Model

Now considering the system model for CHSTN under the CA STBC-NOMA scheme, wherein during the caching phase, ST node *R* can cache up to *C* files out of the total *N* content files (*C*<*N*) of the library at satellite node *S* while following the MPC-based caching scheme. Thus, relying on the Zipf distribution for the content popularity model [13], the probability of requesting *k*-th file can be given as $f_k = (k^\lambda \sum_{k_1=1}^N k_1^{-\lambda})^{-1}$ with λ be the popularity parameter whose higher value refers to the request on the high popularity files. We assume here that the file popularity is provided by an intelligent algorithm based on historical demands and user behavior. Hereby, after the requesting phase, user D_p gets the

required content either directly from the relay through super-posed signal (in one time phase) or from satellite based on the CF STBC-NOMA scheme.

It is noteworthy that we follow independent and identically distributed channels from multiple antennas in satellite and relay by considering that they are lying in a close vicinity [4]. As a result, for convenience, we drop the superscript l from all the notations of the related channel parameters in the succeeding sections.

III. OUTAGE PERFORMANCE OF PRIMARY NETWORK

In this section, we investigate the performance of the primary satellite network by deriving the OP expressions under the proposed CF/CA STBC-NOMA schemes, and thereby provide useful insights by fetching the diversity orders from the asymptotic OP expressions.

A. CF STBC-NOMA Scheme

1) OP Analysis: For a given SINR threshold γ_{d_p}, the OP of user D_p under the CF STBC-NOMA scheme can be written while utilizing maximal-ratio combining (MRC) as

$$P_{\text{out}}^{x_{d_p},\text{CF}} = \underbrace{\Pr\left[\Lambda_{sr,x_{d_p}} \geq \gamma_{d_p}, \left(\Lambda_{sd_p,x_{d_p}} + \Lambda_{rd_p,x_{d_p}}\right) < \gamma_{d_p}\right]}_{P_1}$$
$$+ \underbrace{\Pr\left[\Lambda_{sr,x_{d_p}} < \gamma_{d_p}, \Lambda_{sd_p,x_{d_p}} < \gamma_{d_p}\right]}_{P_2}, \quad (5)$$

where $\gamma_{d_p} = 2^{2R_{d_p}} - 1$ with R_{d_p} being the target rate for user D_p. Herein, P_1 can be obtained as $P_1 = I_1 I_2$ with $I_1 = \Pr[\Lambda_{sr,x_{d_p}} \geq \gamma_{d_p}] = 1 - F_{\Lambda_{sr,x_{d_p}}}(\gamma_{d_p})$, $I_2 = \Pr[\Lambda_{d_p,x_{d_p}} < \gamma_{d_p}] = F_{\Lambda_{d_p,x_{d_p}}}(\gamma_{d_p})$ with $\Lambda_{d_p,x_{d_p}} = \Lambda_{sd_p,x_{d_p}} + \Lambda_{rd_p,x_{d_p}}$. Whereas, P_2 can be computed as $P_2 = I_3 I_4$ with $I_3 = 1 - I_1$ and $I_4 = \Pr[\Lambda_{sd_p,x_{d_p}} < \gamma_{d_p}] = F_{\Lambda_{sd_p,x_{d_p}}}(\gamma_{d_p})$ can be obtained by replacing the subscript r with d_p in each term of I_3. In the above lines, $F_{\cdot}(\cdot)$ specifies the cumulative distribution function (CDF). Next, I_1 can be derived as given below in Theorem 1.

Theorem 1: The analytical term I_1 can be derived as

$$I_1 = \sum_{\kappa_1=0}^{m_{sr}-1} \sum_{\kappa_2=0}^{m_{sr}-1} \sum_{m=0}^{\kappa_1} \sum_{g=0}^{m} \alpha_r^2 \frac{\zeta(\kappa_1)\zeta(\kappa_2)}{(\tilde{\eta}_s)^{\kappa_1+\kappa_2+2}} \frac{\kappa_1!}{m!} \binom{m}{g}(-1)^g$$
$$\times \left(\frac{\tilde{\eta}_s}{\beta_r - \delta_r}\right)^{\kappa_1-m+1} e^{-\frac{(\beta_r-\delta_r)}{\tilde{\eta}_s}\gamma_{d_p}} \frac{\gamma_{d_p}^{m+\kappa_2+1}}{g+\kappa_2+1}$$
$$+ \sum_{\kappa_1=0}^{m_{sr}-1} \sum_{\kappa_2=0}^{m_{sr}-1} \alpha_r^2 \frac{\zeta(\kappa_1)\zeta(\kappa_2)\kappa_1!}{(\beta_r-\delta_r)^{\kappa_1+\kappa_2+2}} \Gamma\left(\kappa_2+1, \frac{\beta_r-\delta_r}{\tilde{\eta}_s}\gamma_{d_p}\right), \quad (6)$$

with $\Gamma(\cdot, \cdot)$ being the upper incomplete Gamma function [11, eq. (8.350.2)].

Proof: See Appendix A. ∎

Now evaluation of I_2 can be performed by following the L-step staircase approximation approach as in [14]

$$I_2 \approx \sum_{i=0}^{L-1}\left\{F_{\Lambda_{sd_p,x_{d_p}}}\left(\frac{i+1}{L}\gamma_{d_p}\right) - F_{\Lambda_{sd_p,x_{d_p}}}\left(\frac{i}{L}\gamma_{d_p}\right)\right\}$$
$$\times F_{\Lambda_{rd_p,x_{d_p}}}\left(\frac{L-i}{L}\gamma_{d_p}\right), \quad (7)$$

where $F_{\Lambda_{rd_p,x_{d_p}}}(\cdot)$ is given in the following lemma.

Lemma 1: The CDF term $F_{\Lambda_{rd_p,x_{d_p}}}(\cdot)$ can be expressed as

$$F_{\Lambda_{rd_p,x_{d_p}}}(x) = 1 - \frac{1}{\Gamma(m_{rd_p})}\Gamma\left(m_{rd_p}, \frac{m_{rd_p}x}{\Omega_{rd_p}\tilde{\eta}_r\theta_x}\right)$$
$$- \sum_{m=0}^{m_{rd_p}-1} \sum_{g=0}^{m} \frac{(-1)^g(g+m_{rd_p})^{-1}}{m!\,\Gamma(m_{rd_p})}\binom{m}{g}e^{-\frac{m_{rd_p}x}{\Omega_{rd_p}\tilde{\eta}_r\theta_x}}$$
$$\left(\frac{m_{rd_p}x}{\Omega_{rd_p}\tilde{\eta}_r\theta_x}\right)^{m+m_{rd_p}}, \quad (8)$$

with $\theta_x = (1-\rho) - \rho x$.

Proof: The proof is similar to that of Theorem 1. ∎

2) Asymptotic OP Analysis: To fetch further insights, we derive the asymptotic OP expression for the primary network under the CF STBC-NOMA scheme at high SNR ($\eta_s, \eta_r \to \infty$, with $\frac{\eta_s}{\eta_r}$ be the constant). Following the preceding section, the asymptotic OP expression can be written as

$$P_{\text{out,asy}}^{x_{d_p},\text{CF}} = I_1^{\text{asy}} I_2^{\text{asy}} + I_3^{\text{asy}} I_4^{\text{asy}}. \quad (9)$$

We first focus on solving the analytical terms I_1^{asy}, I_2^{asy} and therein $F_{\Lambda_{rd_p,x_{d_p}}}^{\text{asy}}(\cdot)$, which are derived in Theorem 2.

Theorem 2: The analytical terms I_1^{asy} and $F_{\Lambda_{rd_p,x_{d_p}}}^{\text{asy}}(\cdot)$ can be given as

$$I_1^{\text{asy}} = 1 - \sum_{\kappa_1=0}^{m_{sr}-1} \sum_{\kappa_2=0}^{m_{sr}-1} \sum_{m=0}^{\kappa_1+1} \alpha_r^2 \frac{\zeta(\kappa_1)\zeta(\kappa_2)}{(\tilde{\eta}_s)^{\kappa_1+\kappa_2+2}}\binom{\kappa_1+1}{m}$$
$$\times (-1)^m \frac{\gamma_{d_p}^{\kappa_1+\kappa_1+2}}{(\kappa_1+1)(m+\kappa_2+1)}, \quad (10)$$

$$F_{\Lambda_{rd_p,x_{d_p}}}^{\text{asy}}(x) = \sum_{m=0}^{m_{rd_p}} \binom{m_{rd_p}}{m} \frac{(-1)^m(m+m_{rd_p})^{-1}}{m_{rd_p}(\Gamma(m_{rd_p}))^2}\left(\frac{m_{rd_p}x}{\Omega_{rd_p}\tilde{\eta}_r\theta_x}\right)^{2m_{rd_p}}. \quad (11)$$

Proof: Proof of Theorem 2 can be followed using the steps as in [2, Appendix D]. ∎

In (9), $I_3^{\text{asy}} = 1 - I_1^{\text{asy}}$ and I_4^{asy} can be computed by replacing the subscript r with d_p in each term of I_3^{asy}. Expression for I_2^{asy} can be obtained with the help of (11) and I_4^{asy}, and then incorporating them into (7).

B. CA STBC-NOMA Scheme

1) OP Analysis: Section II-D specifies two possible communication scenarios for the primary user D_p depending on the contents cached at ST node R. Accordingly, the OP related to the content file in each scenario depends on the popularity profile. Thus, the overall OP can be written as the sum of OP multiplied by their popularity profiles in each scenario as

$$P_{\text{out}}^{x_{d_p},\text{CA}} = P_{\text{out}}^{x_{d_p},(a)} \sum_{i=1}^{C} f_i + P_{\text{out}}^{x_{d_p},(b)} \sum_{i=C+1}^{N} f_i, \quad (12)$$

where $P_{\text{out}}^{x_{d_p},(a)}$ can be referred from (8) on substituting $x = \gamma'_{d_p}$ with $\gamma'_{d_p} = 2^{R_{d_p}} - 1$ and $P_{\text{out}}^{x_{d_p},(b)}$ can be followed through (5).

2) Asymptotic OP Analysis: Herein, (12) can be approximated at high SNR to provide asymptotic OP expression of the primary network under the CA STBC-NOMA scheme as

$$P_{\text{out,asy}}^{x_{d_p},\text{CA}} = P_{\text{out,asy}}^{x_{d_p},(a)} \sum_{i=1}^{C} f_i + P_{\text{out,asy}}^{x_{d_p},(b)} \sum_{i=C+1}^{N} f_i, \quad (13)$$

with $P_{\text{out,asy}}^{x_{d_p},(a)} = F_{\Lambda_{rd_p},x_{d_p}}^{\text{asy}}(\gamma'_{d_p})$ and $P_{\text{out,asy}}^{x_{d_p},(b)}$ can be written as (9).

Remark 1: Following (9) and (13), after inserting the expressions for associated terms, one can manifest the diversity order of the primary satellite network under the CF STBC-NOMA and CA STBC-NOMA schemes as $2 + \min(2, 2\, m_{rd_p})$ and $\min(2\, m_{rd_p}, 2 + \min(2, 2\, m_{rd_p}))$, respectively. For this, we observe the dominant terms at high SNR, which are reflected by the minimum power raised to $\frac{1}{\text{SNR}}$. Importantly, these diversity orders are higher than obtained in [1], i.e., $\min(1, m_{rd_p})$.

IV. OUTAGE PERFORMANCE OF SECONDARY NETWORK

This section aims to derive the OP expressions for the secondary terrestrial network under the proposed CF/CA STBC-NOMA schemes, and thereby presents the corresponding realizable diversity orders through asymptotic analysis.

A. CF STBC-NOMA Scheme

1) OP Analysis: For a given SINR threshold γ_{d_q}, the OP of user D_q under the CF STBC-NOMA scheme can be written as

$$P_{\text{out}}^{x_{d_q},\text{CF}} = \Pr\left[\Lambda_{sr,x_{d_p}} \geq \gamma_{d_p}, \Lambda_{rd_q,x_{d_q}} < \gamma_{d_q}\right] + \Pr\left[\Lambda_{sr,x_{d_p}} < \gamma_{d_p}\right]$$
$$= I_1 F_{\Lambda_{rd_q},x_{d_q}}(\gamma_{d_q}) + (1 - I_1), \qquad (14)$$

where $\gamma_{d_q} = 2^{2R_{d_q}} - 1$, with R_{d_q} being the target rate for user D_q. In (14), $P_{\text{out}}^{x_{d_q},\text{CF}}$ is evaluated by deriving the expression for CDF term $F_{\Lambda_{rd_q},x_{d_q}}(\gamma_{d_q})$ as given in Theorem 3.

Theorem 3: The CDF $F_{\Lambda_{rd_q},x_{d_q}}(\gamma_{d_q})$ under hybrid satellite-terrestrial channels can be expressed as $F_{\Lambda_{rd_q},x_{d_q}}(\gamma_{d_q}) = 1 - (\psi_1(\gamma_{d_q}) + \psi_2(\gamma_{d_q}))$, where $\psi_1(\gamma_{d_q})$ and $\psi_2(\gamma_{d_q})$ are provided as

$$\psi_1(\gamma_{d_q}) = \sum_{m=0}^{m_{rd_q}-1} \sum_{g=0}^{m} \sum_{u=0}^{m+m_{rd_q}} \sum_{v=0}^{m+m_{rd_q}-u} \frac{(-1)^g}{m!\, \Gamma(m_{rd_q})} \left(\frac{m_{D_q}}{\Omega_{D_q}\widetilde{\eta_r}}\right)^{2m_{D_q}}$$
$$\times \binom{m}{g}\binom{m+m_{rd_q}}{u}\binom{m+m_{rd_q}-u}{v}\frac{(T_2)^{m+m_{rd_q}-u-v}}{(g+m_{rd_q})}$$
$$\times \left(\frac{m_{rd_q}}{\Omega_{rd_q}\widetilde{\eta_r}}\right)^{m+m_{rd_q}} \frac{\Gamma(u+m_{D_q})\Gamma(v+m_{D_q})}{(T_1)^{-(u+v)}(\Gamma(m_{D_q}))^2} \frac{e^{-\frac{m_{rd_q}T_2}{\Omega_{rd_q}\widetilde{\eta_r}}}}{(T_3)^{u+v+2m_{D_q}}}, \qquad (15)$$

$$\psi_2(\gamma_{d_q}) = \sum_{m=0}^{m_{rd_q}-1} \sum_{g=0}^{m} \sum_{u=0}^{m-g} \left(\frac{m_{D_q}}{\Omega_{D_q}\widetilde{\eta_r}}\right)^{2m_{D_q}} \binom{m-g}{u}\left(\frac{m_{rd_q}}{\Omega_{rd_q}\widetilde{\eta_r}}\right)^{m}$$
$$\times \binom{m}{g}\frac{(T_2)^{m-g-u}}{(T_1)^{-(g+u)}}\frac{\Gamma(g+m_{D_q})\Gamma(u+m_{D_q})}{m!(\Gamma(m_{D_q}))^2} \frac{e^{-\frac{m_{rd_q}T_2}{\Omega_{rd_q}\widetilde{\eta_r}}}}{(T_3)^{u+g+2m_{D_q}}}, \qquad (16)$$

with $T_1 = \frac{(1-\rho)}{\rho}\gamma_{d_q}$, $T_2 = \frac{\gamma_{d_q}}{\rho}$, and $T_3 = \frac{m_{rd_q}}{\Omega_{rd_q}\eta_r}T_1 + \frac{m_{D_q}}{\Omega_{D_q}\widetilde{\eta_r}}$.

Proof: See Appendix B. ∎

2) Asymptotic OP Analysis: To obtain the asymptotic OP expression of the secondary network, we approximate (14) at high SNR as

$$P_{\text{out,asy}}^{x_{d_q},\text{CF}} = I_1^{\text{asy}} F_{\Lambda_{rd_q},x_{d_q}}^{\text{asy}}(\gamma_{d_q}) + (1 - I_1^{\text{asy}}), \qquad (17)$$

where $F_{\Lambda_{rd_q},x_{d_q}}^{\text{asy}}(\gamma_{d_q})$ can be computed using Lemma 2.

Lemma 2: The CDF term $F_{\Lambda_{rd_q},x_{d_q}}^{\text{asy}}(\gamma_{d_q})$ can be obtained as

$$F_{\Lambda_{rd_q},x_{d_q}}^{\text{asy}}(\gamma_{d_q}) = \sum_{m=0}^{m_{rd_q}} \sum_{g=0}^{2m_{rd_q}} \sum_{s=0}^{2m_{rd_q}-g} \frac{(-1)^m(m+m_{rd_q})^{-1}}{m_{rd_q}(\Gamma(m_{rd_q}))^2}$$
$$\times \binom{m_{rd_q}}{m}\binom{2m_{rd_q}}{g}\binom{2m_{rd_q}-g}{s}\left(\frac{m_{rd_q}}{\Omega_{rd_q}\widetilde{\eta_r}}\right)^{2m_{rd_q}}$$
$$\times \frac{(T_1)^{g+s}}{(T_2)^{g+s-2m_{rd_q}}}\left(\frac{\Omega_{D_q}\widetilde{\eta_r}}{m_{D_q}}\right)^{g+s}\frac{\Gamma(g+m_{D_q})\Gamma(s+m_{D_q})}{(\Gamma(m_{D_q}))^2}. \qquad (18)$$

Proof: The proof is similar to that of Theorem 2. ∎

B. CA STBC-NOMA Scheme

1) OP Analysis: Referring to Section III-B, the overall OP for CA STBC-NOMA can be written as

$$P_{\text{out}}^{x_{d_q},\text{CA}} = P_{\text{out}}^{x_{d_q},(a)} \sum_{i=1}^{C} f_i + P_{\text{out}}^{x_{d_q},(b)} \sum_{i=C+1}^{N} f_i, \qquad (19)$$

where $P_{\text{out}}^{x_{d_q},(a)} = F_{\Lambda_{rd_q},x_{d_q}}(\gamma'_{d_q})$, which can be directed from Theorem 3 on substituting $\gamma_{d_q} = \gamma'_{d_q}$, where $\gamma'_{d_q} = 2^{R_{d_q}} - 1$. Further, $P_{\text{out}}^{x_{d_p},(b)} = P_{\text{out}}^{x_{d_q},\text{CF}}$, and can be followed using (14).

2) Asymptotic OP Analysis: To provide asymptotic OP expression of the secondary network under the CA STBC-NOMA scheme, (19) can be approximated at high SNR as

$$P_{\text{out,asy}}^{x_{d_q},\text{CA}} = P_{\text{out,asy}}^{x_{d_q},(a)} \sum_{i=1}^{C} f_i + P_{\text{out,asy}}^{x_{d_q},(b)} \sum_{i=C+1}^{N} f_i, \qquad (20)$$

with $P_{\text{out,asy}}^{x_{d_q},(a)} = F_{\Lambda_{rd_q},x_{d_q}}^{\text{asy}}(\gamma'_{d_q})$ and $P_{\text{out,asy}}^{x_{d_q},(b)}$ can be written as (17).

Remark 2: Following (17) and (20), after substituting the expressions for associated terms, one can assess the diversity order of the secondary terrestrial network under both CF STBC-NOMA and CA STBC-NOMA schemes as zero, owing to the realistic ipSIC situation. On the contrary, for perfect SIC case, one can find the respective diversity orders under the CF STBC-NOMA and CA STBC-NOMA schemes as $\min(2, 2\, m_{rd_q})$ and $\min(2\, m_{rd_q}, \min(2, 2\, m_{rd_q}))$.

V. NUMERICAL AND SIMULATION RESULTS

For numerical results, we set $\eta_s = \eta_r = \eta$ as the transmit SNR, $R_{d_p} = R_{d_q} = 0.5$ so that $\gamma'_{d_p} = 0.414$, $\gamma_{d_p} = 1$, $\gamma_{d_q} = 1, \gamma'_{d_q} = 0.414$, $\Omega_{rd_p} = \Omega_{rd_q} = 1$, $\rho = 0.3$ [1], and $L = 100$ [14]. Also, we set the satellite parameters as $(m_{si}, b_{si}, \Omega_{si}) = (2, 0.063, 0.0005)$ and $(m_{si}, b_{si}, \Omega_{si}) = (5, 0.251, 0.279)$, $i \in \{r, d_p, d_q\}$, for heavy shadowing (HS) and average shadowing (AS) scenarios, respectively [14]. The parameters related to considered caching scheme are set as $N = 200$, $C = 20$, and $\lambda = 2$ [9]. For notation simplicity, we mark CF STBC-NOMA, CA STBC-NOMA, and Simulation as CF, CA, and Sim., respectively, in the various figures.

Fig. 1(a) depicts the OP versus SNR curves for primary network while setting $m_{rd_p} = 1$ and $m_{rd_p} = 2$. First, it can be ensured that analytical and asymptotic curves are well matched with the exact simulation results. As such, it can be seen that the CA scheme outperforms the CF scheme in the
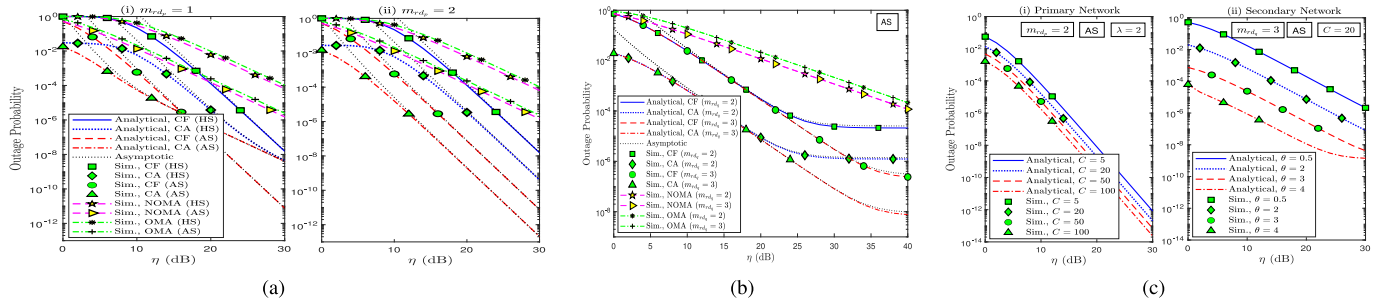
Fig. 1. (a) OP versus SNR curves for primary network; (b) OP versus SNR curves for secondary network; (c) Impact of caching parameters on outage performance.

low SNR region under $m_{rd_p} = 1$, and throughout the SNR region under $m_{rd_p} = 2$. This behaviour can be readily verified through the diversity orders of $2 + \min(2, 2\,m_{rd_p})$ and $\min(2\,m_{rd_p}, 2 + \min(2, 2\,m_{rd_p}))$ from the respective curves of CF and CA schemes. Further, the outage curves corresponding to the proposed CF/CA STBC-NOMA schemes illuminate better performance as compared to the simulation curves of benchmark NOMA and OMA schemes. Moreover, the overall outage performance relatively improves when satellite links are encountered with AS than its HS counterpart.

Fig. 1(b) illustrates the OP curves for secondary network against SNR under the setting $m_{rd_q} = 2$ and $m_{rd_q} = 3$. It can be visualized from the respective curves that the CA scheme outperforms the CF scheme owing to the efficient utilization of available spectrum resources based on the primary contents cached at the relay. Further, the error floors are observed for the proposed CF/CA schemes that are associated with the ipSIC situations and resulting in zero diversity order.

Fig. 1(c) demonstrates the impacts of caching parameters C and λ on the outage performance of primary and secondary networks, respectively. Apparently, the outage performance improves while increasing the cache size C. This is primarily due to the efficient use of available spectrum resources while fetching the contents by user D_p directly from the relay itself. Moreover, the outage performance ameliorates as the value of λ increases. As such, a higher value of λ refers to the lower-index files with high popularity and can be stored in the relay with limited cache capacity.

VI. Conclusion

We investigated an overlay-based CHSTN system wherein a secondary terrestrial network cooperates with a primary satellite network for dynamic spectrum access. Importantly, the considered analytical framework deploys the NOMA and conventional Alamouti STBC techniques for the signal transmissions and ST has built-in cache capability to store the popular contents of the primary network. For this, we proposed the novel CF/CA STBC-NOMA schemes and correspondingly assessed the outage performance. Hereby, a comparison with benchmark stand-alone NOMA and OMA schemes revealed that the proposed CF/CA STBC-NOMA schemes ameliorate the performance of CHSTN by utilizing the spectrum resources efficiently.

Appendix A

The analytical term I_1 can be expressed using (5) as

$$I_1 = \Pr\left[\left(\Lambda_{sr}^1 + \Lambda_{sr}^2\right) \geq \gamma_{d_p}\right], \qquad (21)$$

which can be further computed as

$$I_1 = \int_0^{\gamma_{d_p}} \left(\int_{\gamma_{d_p}-y}^\infty f_{\Lambda_{sr}^1}(x)\,dx\right) f_{\Lambda_{sr}^2}(y)\,dy$$
$$+ \int_{\gamma_{d_p}}^\infty \left(\int_0^\infty f_{\Lambda_{sr}^1}(x)\,dx\right) f_{\Lambda_{sr}^2}(y)\,dy. \qquad (22)$$

On invoking the associated PDF $f_{\Lambda_{sr}^l}(\cdot)$ from [2, eq. (6)], and then simplifying the integrals using [11, eqs. (3.351.2) and (3.351.3)] and binomial expansion [11, eq. (1.111)], one can grab the desired result in (6).

Appendix B

Following the (14), the CDF term $F_{\Lambda_{rd_q}, x_{d_q}}(\gamma_{d_q})$ can be written with the aid of (4) as

$$F_{\Lambda_{rd_q}, x_{d_q}}(\gamma_{d_q}) = 1 - \Pr\left[\Lambda_{rd_q}^1 \geq T_1\left(\Lambda_{D_q}^1 + \Lambda_{D_q}^2\right) - \Lambda_{rd_q}^2 + T_2\right]$$
$$= 1 - \left(\psi_1(\gamma_{d_q}) + \psi_2(\gamma_{d_q})\right), \qquad (23)$$

where $\psi_1(\gamma_{d_q})$ and $\psi_2(\gamma_{d_q})$ can be evaluated as (15) and (16) by following the similar steps as in Appendix A.

References

[1] X. Zhang et al., "Outage performance of NOMA-based cognitive hybrid satellite-terrestrial overlay networks by amplify-and-forward protocols," *IEEE Access*, vol. 7, pp. 85372–85381, 2019.

[2] V. Singh and P. K. Upadhyay, "Exploiting cache-free/cache-aided TWR-NOMA in cognitive hybrid satellite-terrestrial networks," *IEEE Trans. Veh. Technol.*, vol. 71, no. 2, pp. 1778–1793, Feb. 2022.

[3] M. N. Jamal et al., "Efficient nonorthogonal multiple access: Cooperative use of distributed space-time block coding," *IEEE Veh. Technol. Mag.*, vol. 13, no. 4, pp. 70–77, Dec. 2018.

[4] M. K. Arti and S. K. Jindal, "OSTBC transmission in shadowed-Rician land mobile satellite links," *IEEE Trans. Veh. Technol.*, vol. 65, no. 7, pp. 5771–5777, Jul. 2016.

[5] S. M. Alamouti, "A simple transmit diversity technique for wireless communications," *IEEE J. Sel. Areas Commun.*, vol. 16, no. 8, pp. 1451–1458, Oct. 1998.

[6] Y. Dhungana, N. Rajatheva, and C. Tellambura, "Dual hop MIMO OSTBC for LMS communication," *IEEE Wireless Commun. Lett.*, vol. 1, no. 2, pp. 105–108, Apr. 2012.

[7] Y. Ruan et al., "Performance analysis of hybrid satellite-terrestrial cooperative networks with distributed Alamouti code," in *Proc. IEEE Veh. Technol. Conf. (VTC) Spring*, Nanjing, China, May 2016, pp. 1–5.

[8] T. X. Vu et al., "Modeling and implementation of 5G edge caching over satellite," *Int. J. Satell. Commun.*, vol. 38, no. 5, pp. 395–406 Jan. 2020.

[9] K. An et al., "On the performance of cache-enabled hybrid satellite-terrestrial relay networks," *IEEE Wireless Commun. Lett.*, vol. 8, no. 5, pp. 1506–1509, Oct. 2019.

[10] *Digital Video Broadcasting (DVB); System Specifications for Satellite Services to Handheld Devices (SH) Below 3 GHz*, ETSI Standard TS 102 585 V1.1.2, Apr. 2008.

[11] I. S. Gradshteyn and I. M. Ryzhik, *Tables of Integrals, Series and Products*, 7th ed. San Diego, CA, USA: Academic, 2007.

[12] L. Luo et al., "Performance analysis of overlay cognitive NOMA systems with imperfect successive interference cancellation," *IEEE Trans. Commun.*, vol. 68, no. 8, pp. 4709–4722, Aug. 2020.

[13] L. Breslau et al., "Web caching and Zipf-like distributions: Evidence and implications," in *Proc. IEEE Int. Conf. Computer Commun. (INFOCOM)*, San Diego, CA, USA, Mar. 1999, pp. 1–8.

[14] P. K. Sharma et al., "Performance analysis of overlay spectrum sharing in hybrid satellite-terrestrial systems with secondary network selection," *IEEE Trans. Wireless Commun.*, vol. 16, no. 10, pp. 6586–6601, Oct. 2017.